Acta Crystallographica Section F
Structural Biology and Crystallization Communications
ISSN 1744-3091

Production, crystallization and preliminary X-ray analysis of CTP:inositol-1-phosphate cytidylyltransferase from *Archaeoglobus fulgidus*

José A. Brito, Nuno Borges, Helena Santos and Margarida Archer*

Instituto de Tecnologia Química e Biológica, Universidade Nova de Lisboa, Avenida da República, EAN, 2780-157 Oeiras, Portugal

Correspondence e-mail: archer@itqb.unl.pt

Received 9 July 2010
Accepted 13 August 2010

Archaeoglobus fulgidus, a hyperthermophilic archaeon, accumulates di-*myo*-inositol phosphate (DIP) in response to heat stress. Recently, the pathway for biosynthesis of DIP has been elucidated in this organism and involves a bifunctional enzyme that contains two domains: CTP:inositol-1-phosphate cytidylyltransferase (IPCT) as a soluble domain and di-*myo*-inositol-1,3′-phosphate-1-phosphate synthase (DIPPS) as a membrane domain. Here, the expression, purification, crystallization and preliminary X-ray diffraction analysis of the IPCT domain from *A. fulgidus* in the apo form are reported. The crystals diffracted to 2.4 Å resolution using a synchrotron source and belonged to the orthorhombic space group $P2_12_12$, with unit-cell parameters a = 154.7, b = 83.9, c = 127.7 Å.

1. Introduction

Di-*myo*-inositol phosphate (DIP) is a compatible solute that is widespread amongst microorganisms adapted to hot environments and has never been found in mesophilic organisms (Santos *et al.*, 2007). In general, DIP increases notably in response to heat stress, suggesting that it plays a role in thermoadaptation (Borges *et al.*, 2010).

A novel pathway for DIP synthesis, which involves a phosphorylated intermediate, has been proposed by Borges *et al.* (2006) and has been fully corroborated by the subsequent identification and characterization of the key genes and enzymes (Rodrigues *et al.*, 2007; Rodionov *et al.*, 2007). The first step is catalysed by CTP:inositol-1-phosphate cytidylyltransferase (IPCT) and involves the condensation of L-*myo*-inositol-1-phosphate and CTP to yield CDP-inositol; this product is coupled to a second molecule of L-*myo*-inositol-1-phosphate to yield the phosphorylated intermediate di-*myo*-inositol-1,3′-phosphate-1-phosphate (DIPP) in a reaction catalyzed by DIPP synthase; finally, DIPP is dephosphorylated to DIP by the action of a phosphatase.

The IPCT and DIPPS (di-*myo*-inositol-1,3′-phosphate-1-phosphate synthase) activities are present in a single polypeptide chain in *Archaeoglobus fulgidus* and in most organisms that are known to accumulate DIP, although the two activities are separated in *Hyperthermus butylicus* and *Thermotoga* spp. The C-terminal DIPPS domain is believed to be membrane-associated, with three predicted transmembrane segments (Rodrigues *et al.*, 2007)

Attempts to produce this novel bifunctional enzyme from *A. fulgidus* in heterologous systems showed poor yields. Moreover, the activity of the DIPPS domain was invariably lost during the purification procedure, probably reflecting its membrane association. Therefore, we decided to proceed with characterization of the soluble IPCT domain. Here, we report the expression, purification, crystallization and preliminary X-ray analysis of IPCT from *A. fulgidus*.

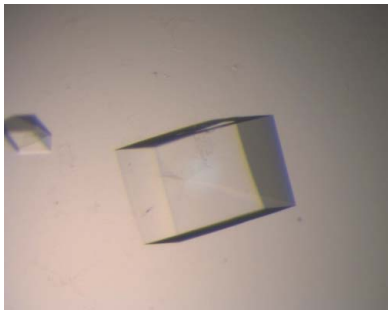

2. Materials and methods

2.1. Cloning, expression and purification of the IPCT domain from *A. fulgidus*

In order to define the IPCT domain in the bifunctional IPCT/DIPPS from *A. fulgidus* (AF0263), the amino-acid sequence of

AF0263 (436 amino acids) was aligned with the monofunctional IPCT and DIPPS sequences from *H. butylicus*, *Aeropyrum pernix*, *Thermotoga maritima* and *T. petrophila* using the program *ClustalW* (Larkin *et al.*, 2007). On the basis of this analysis, the IPCT domain of the *A. fulgidus* bifunctional IPCT/DIPPS was identified as the N-terminal polypeptide starting with MINVDG and continuing to residue 232. This domain was cloned and expressed in *Escherichia coli*. The chromosomal DNA from *A. fulgidus* was isolated according to Ramakrishnan & Adams (1995). The IPCT domain was amplified by PCR using *Pfu* DNA polymerase (Fermentas). The set of primers used for the amplification were IPCT-F (5′-CGG**CATATG**ATAAATGTTGACGGAG-3′; the *Nde*I restriction site is shown in bold) and IPCT-R (5′-CGG**CTCGAG**TTACAAGGCTCTATTAG-3′; the *Xho*I restriction site is shown in bold). The PCR product was cloned in the pET19b plasmid (Novagen) between the *Nde*I and *Xho*I sites. The correct nucleotide sequence of the construct was confirmed by DNA sequencing (Agowa, Germany). *E. coli* BL21(DE3)pLys cells bearing the construct were grown at 310 K in LB medium supplemented with ampicillin (100 mg ml^{-1}) and chloramphenicol (34 mg ml^{-1}) to an $A_{600\,\mathrm{nm}}$ of 0.6 and were induced with 1 m*M* IPTG for 4 h.

The cells were collected by centrifugation, suspended in 20 m*M* Tris–HCl plus 10 m*M* $MgCl_2$ pH 7.6 and disrupted in a French press. IPCT was purified from heat-treated cell extracts (30 min at 343 K) using a His-Trap column and the histidine tag was cleaved with enterokinase (18 h at 310 K). Subsequently, the enterokinase-treated sample was applied onto a second His-Trap column. The flowthrough fraction was dialyzed overnight against 50 m*M* Tris–HCl pH 7.6 and concentrated in a Centricon (10 000 molecular-weight cutoff). A final polishing step was performed by applying the IPCT onto a Superdex G75 gel-filtration column. The purity of the final protein preparation was evaluated by 10% SDS–PAGE.

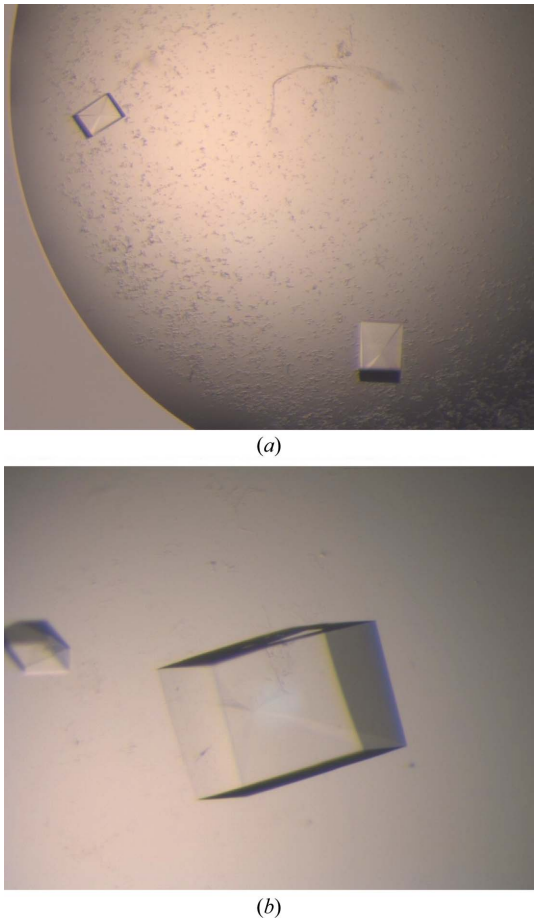

(*a*)

(*b*)

Figure 1
IPCT crystals grown in 1.2 *M* trisodium citrate dihydrate, 100 m*M* HEPES pH 7.2 and 10 m*M* $MgCl_2$. The crystals took approximately two weeks to appear and grew to dimensions of 0.15 × 0.15 × 0.15 mm.

Table 1
Data-collection and processing statistics.

Values in parentheses are for the highest resolution shell.

	IPCT	IPCT–$HgCl_2$
X-ray source	Beamline ID23-1, ESRF	Beamline ID14-2, ESRF
Wavelength (Å)	1.067	0.933
Space group	$P2_12_12$	$P2_12_12$
Unit-cell parameters (Å)	a = 154.7, b = 83.9, c = 127.7	a = 153.6, b = 83.5, c = 127.8
Resolution (Å)	48.3–2.4 (2.53–2.40)	49.3–2.9 (3.10–2.90)
$R_{\rm merge}$	0.050 (0.426)	0.080 (0.597)
$R_{\rm meas}$	0.058 (0.504)	0.112 (0.780)
$\langle I/\sigma(I)\rangle$	13.4 (2.3)	12.2 (2.6)
No. of reflections		
Observed	224153	116728
Unique	64618	32022
Multiplicity	3.5 (3.5)	3.6 (3.7)
Completeness (%)	98.8 (99.5)	97.4 (99.2)

2.2. IPCT crystallization and cryo-conditions

The protein sample was concentrated to about 12 mg ml^{-1} in 10 m*M* HEPES buffer pH 7.5 using an Amicon YM-10 concentrator device (Millipore). Initial crystallization screenings were performed by vapour diffusion using a Cartesian robot dispensing system ('mini-bee'; Genomic Solutions) and the commercially available screens Classics I and II Suites (Qiagen) and SaltRx (Hampton Research). The flat-bottom 96-well plates (Greiner Bio-One) contained sitting drops consisting of 100 nl protein sample mixed with 100 nl precipitant solution that were equilibrated against a reservoir consisting of 90 µl precipitant solution. The sealed plates were incubated at room temperature (293 K).

Initial crystalline material appeared in several conditions from the different screens that mainly contained salts (*i.e.* sodium/potassium phosphate or sodium malonate, citrate or formate) as precipitants at low pH values (4.5–6). Optimization of these conditions included grid screens surrounding the crystallization hits using the hanging-drop vapour-diffusion technique. Drops consisted of 1.5 µl protein solution and 1.5 µl precipitant solution and were equilibrated against 500 µl reservoir solution in 24-well EasyXtal Tool plates (Qiagen) at room temperature (293 K). The optimized crystallization condition yielding diffraction-quality crystals of IPCT consisted of 1.2–1.4 *M* trisodium citrate dihydrate, 100 m*M* HEPES pH 6.8–7.2 and 10 m*M* $MgCl_2$.

2.3. X-ray diffraction experiments

A single crystal with approximate dimensions of 0.15 × 0.15 × 0.15 mm (Fig. 1) was used for data collection at cryogenic temperature. Crystallization buffer/mother liquor supplemented with 10% glycerol was used as a cryoprotectant and the crystal was flash-cooled at 100 K in a nitrogen-gas steam (Oxford Cryosystems 700). X-ray diffraction images were collected using ADSC Q4 and ADSC Q315R CCD detectors on ESRF beamlines ID14-2 and ID23-1 (ESRF, Grenoble), respectively. The data were indexed and processed using *XDS* (Kabsch, 2010) and scaled with *SCALA* from the *CCP*4 program package (Evans, 1997; Collaborative Computational Project, Number 4, 1994). The crystals belonged to the orthorhombic space group $P2_12_12$, with unit-cell parameters a = 154.7, b = 83.9, c = 127.7 Å. Data-collection statistics are summarized in Table 1. Calculation of

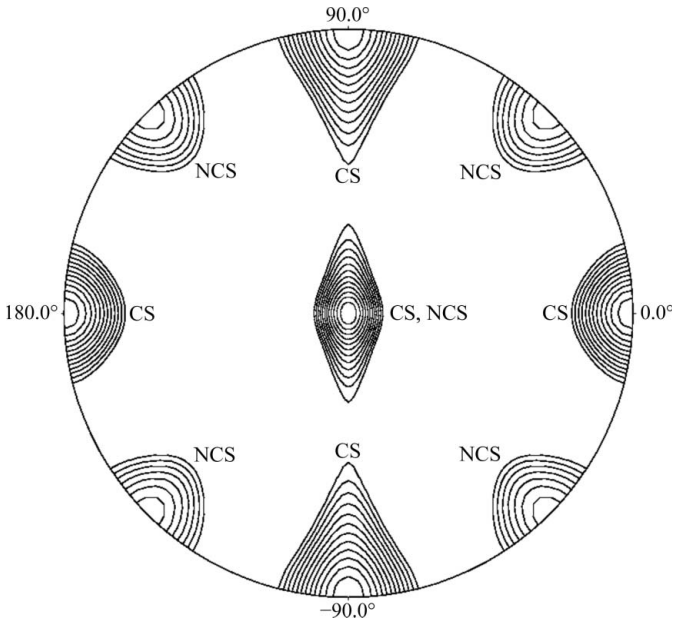

Figure 2
Self-rotation Patterson-function plot for IPCT in the resolution range $3.0 \leq d \leq 15$ Å with integration range $5.0 \leq R \leq 15$ Å. Peaks in the section shown at $\kappa = 180°$ give the orientation of the crystallographic (CS) and noncrystallographic (NCS) twofold rotation axes in the crystal structure. The plot is scaled to a maximum value of 100 and the contours are drawn at five-unit intervals starting at 40. The figure was prepared with the programs *POLARRFN*, *NPO* and *XPLOT*84*DRIVER* (Evans, 1997).

the Matthews coefficient (Matthews, 1968) yielded V_M values of 2.62 $Å^3$ Da^{-1} corresponding to a solvent content of approximately 53% and six molecules in the asymmetric unit or 2.25 $Å^3$ Da^{-1} corresponding to 45% solvent content and seven molecules in the asymmetric unit. Thus, the protein content in the crystal asymmetric unit of IPCT is not clear at this point.

A self-rotation function calculated with the program *POLARRFN* (Evans, 1997) from *CCP*4 (Collaborative Computational Project, Number 4, 1994) indicated the existence of three twofold noncrystallographic symmetry axes (Fig. 2). Two of these are approximately perpendicular to the crystallographic *c* axis, while the third is either coincident or slightly angled relative to it, since no strong non-origin peaks were observed in a native Patterson map (not shown).

A search for potential derivatives was performed by soaking freshly prepared IPCT crystals in crystallization solution containing heavy-atom compound salts [K_2Cl_4Pt, $KAu(CN)_2$ or $HgCl_2$; JBScreen Heavy, Jena Biosciences] at concentrations ranging from 0.5 to 5 m*M* and with incubation times from minutes to several days at room temperature. In addition, a quick soak was also performed with 1 *M* KI for 30 s prior to crystal cryocooling. The programs *SHELXC*/*D*/*E* (Sheldrick, 2008) within *HKL2MAP* (Pape & Schneider, 2004) were used to attempt phasing using the single isomorphous replacement with anomalous scattering method. *SHELXC* was used to prepare the experimental data and *SHELXD* was used to analyze the data sets from the putative derivatives. *SHELXD* indicated clear anomalous signal up to 5 Å resolution for one mercury derivative (5 m*M* $HgCl_2$ for 4 h), but *SHELXE* did not produce an interpretable map. Further analysis is under way to solve the phase problem.

3. Concluding remarks

The crystallization of IPCT is a crucial step towards the elucidation of the catalytic mechanism of this unique enzyme that is able to catalyze the synthesis of CDP-inositol. The occurrence of this metabolite was first disclosed by our group (Borges *et al.*, 2006).

This work was supported by Fundação para a Ciência e a Tecnologia (FCT) through projects PTDC/SAU-NEU/103720/2008 (MA) and PTDC/BIA-MIC/71146/2006 (HS). JAB is the recipient of FCT fellowship BD/30512/2006. We would like to thank the ESRF for financial and technical support for data collection. The authors acknowledge Mafalda Henriques for constructing the expression plasmid and Dr Pedro Matias for help during data collection.

References

Borges, N., Gonçalves, L. G., Rodrigues, M. V., Siopa, F., Ventura, R., Maycock, C., Lamosa, P. & Santos, H. (2006). *J. Bacteriol.* **188**, 8128–8135.
Borges, N., Matsumi, R., Imanaka, T., Atomi, H. & Santos, H. (2010). *J. Bacteriol.* **192**, 191–197.
Collaborative Computational Project, Number 4 (1994). *Acta Cryst.* D**50**, 760–763.
Evans, P. R. (1997). *Proceedings of the CCP4 Study Weekend. Recent Advances In Phasing*, edited by K. S. Wilson, G. Davies, A. W. Ashton & S. Bailey, pp. 97–102. Warrington: Daresbury Laboratory.
Kabsch, W. (2010). *Acta Cryst.* D**66**, 125–132.
Larkin, M. A., Blackshields, G., Brown, N. P., Chenna, R., McGettigan, P. A., McWilliam, H., Valentin, F., Wallace, I. M., Wilm, A., Lopez, R., Thompson, J. D., Gibson, T. J. & Higgins, D. G. (2007). *Bioinformatics*, **23**, 2947–2948.
Matthews, B. W. (1968). *J. Mol. Biol.* **33**, 491–497.
Pape, T. & Schneider, T. R. (2004). *J. Appl. Cryst.* **37**, 843–844.
Ramakrishnan, V. & Adams, M. W. W. (1995). *Archaea: A Laboratory Manual – Thermophiles*, edited by F. T. Robb & A. R. Place, pp. 95–96. New York: Cold Spring Harbor Laboratory Press.
Rodionov, D. A., Kurnasov, O. V., Stec, B., Wang, Y., Roberts, M. F. & Osterman, A. L. (2007). *Proc. Natl Acad. Sci. USA*, **104**, 4279–4284.
Rodrigues, M. V., Borges, N., Henriques, M., Lamosa, P., Ventura, R., Fernandes, C., Empadinhas, N., Maycock, C., da Costa, M. S. & Santos, H. (2007). *J. Bacteriol.* **189**, 5405–5412.
Santos, H., Lamosa, P., Faria, T. Q., Borges, N. & Neves, C. (2007). *Physiology and Biochemistry of Extremophiles*, edited by C. Gerday & N. Glansdorff, pp. 86–104. Washington: American Society for Microbiology.
Sheldrick, G. M. (2008). *Acta Cryst.* A**64**, 112–122.